

ORIGINAL RESEARCH ARTICLE

Gut microbiota-derived endotoxin enhanced the incidence of cardia bifida during cardiogenesis[†]

Jing Zhang^{1#}, Guang Wang^{1#}, Jia Liu^{2#}, Lin-rui Gao¹, Meng Liu¹, Chao-jie Wang¹, Manli Chuai³, Yongping Bao⁴, Ge Li⁵, Rui-man Li², Yu Zhang⁵, Xuesong Yang^{1*}

¹*Division of Histology and Embryology, Key Laboratory for Regenerative Medicine of the Ministry of Education, Medical College, Jinan University, Guangzhou 510632, China.*

²*The First Affiliate Hospital of Jinan University, Guangzhou 510630, China.*

³*Division of Cell and Developmental Biology, University of Dundee, Dundee, DD1 5EH, UK.*

⁴*Norwich Medical School, University of East Anglia, Norwich, Norfolk, UK.*

⁵*Guangdong Laboratory Animals Monitoring Institute, Guangdong Provincial Key Laboratory of Laboratory Animals, Guangzhou, Guangdong 510663, China*

[#]contribute to the work equally

*The corresponding author: X Yang. E-mail: yang_xuesong@126.com Tel: +86(20)85228316

[†]This article has been accepted for publication and undergone full peer review but has not been through the copyediting, typesetting, pagination and proofreading process, which may lead to differences between this version and the Version of Record. Please cite this article as doi: [10.1002/jcp.26175]

Additional Supporting Information may be found in the online version of this article.

Received 5 July 2017; Revised 25 August 2017; Accepted 30 August 2017

Journal of Cellular Physiology

This article is protected by copyright. All rights reserved

DOI 10.1002/jcp.26175

Abstract

Background

Cytotoxicity and inflammation-associated toxic responses could be induced by bacterial lipopolysaccharides (LPS) *in vitro* and *in vivo* respectively. However, the mechanism involved in LPS-induced cardiac malformation in prenatal fetus is still unknown.

Methods and results

In this study, we demonstrated that LPS was induced in gut microbiota imbalance mice, and next, LPS exposure during gastrulation in the chick embryo increased the incidence of cardia bifida. Gene transfection and tissue transplantation trajectory indicated that LPS exposure restricted the cell migration of cardiac progenitors to primary heart field in gastrula chick embryos. *In vitro* explant allograft of GFP-labeled anterior primitive streak demonstrated that LPS treatments could inhibit cell migration. A similar observation was also obtained from the cell migration assay of scratch wounds using primary culture of cardiomyocytes or H9c2 cells. In the embryos exposed to LPS, expressions of Nkx2.5 and GATA5 were disturbed. These genes are associated with cardiomyocyte differentiation when heart tube fusion occurs. Furthermore, pHIS3, C-caspase3 immunohistological staining indicated that cell proliferation decreased, cell apoptosis increased in the heart tube of chick embryo. Meanwhile, *in vivo*, pHIS3 immunohistological staining and Hoechst/PI staining also draw the similar conclusions. The LPS exposure also caused the production of excess ROS, which might damage the cardiac precursor cells of developing embryos. At last, we showed that LPS-induced cardia bifida could be partially rescued through the addition of antioxidants.

Conclusions

Together, these results reveal that excess ROS generation is involved in the LPS-induced defects in heart tube during chick embryo development. This article is protected by copyright. All rights reserved

Key words: Lipopolysaccharides, Chick Embryo, Reactive oxygen species, Heart Tube.

Introduction

Commensal microbiota colonized in the human host have complicated interaction with bacterial communities that offer significant health benefits to that host. Accumulating data indicate the connection between gut bacteria and practically every aspect of human health [1, 2]. The impact that these bacteria exert on our health are mainly due to their imbalance. In the past decade, extensive clinical and basic evidence has shown that the gut microbiota can bring about intestinal inflammation and tumorigenesis as a consequence of complex interactions between the human host and bacteria [3]. These intestinal microbes might also exert physiological influences on gut function, immune maintenance and neurological regulation etc.[4, 5]. The beneficial role of the microbial community could even be presented in morphogenesis, except for the maintenance of host physiological functions [5]. However, the microbes could certainly elicit apathogenic response if there were significant alterations in their compositional balance. It is known that obesity, insulin resistance and the metabolic syndrome could all lead to alteration of gut microbiota, in which acetate plays a key role through regulation of microbiome-brain-beta cell axis [6]. Lipopolysaccharide (LPS) is one of the microbial products leading to the possibility that microbiota-derived LPS might interfere with maternal physiology functions and fetal development [7].

LPS is the major component of the outer membrane of Gram-negative bacteria [8, 9]. Of inflammatory-related signaling pathways, Toll-like receptor (TLR) acts as one of the crucial molecules. TLR4 is an innate immune receptor for LPS, which interacts with LPS binding protein to activate TLR4 signaling through the interaction of LPS with TLR4. Subsequently, TLR4 signaling transduction cascade stimulates PI3K/Akt pathway and NF- κ B signaling to cause biological effect [10]. It has been reported that maternal LPS exposure can negatively affect the process of gametogenesis, embryo implantation, gastrulation and neurulation respectively [11-13]. However, these embryonic phenotypes and the underlying mechanisms caused by maternal LPS are still elusive. In particular, little is known about the cardiac precursor cell migration and cellular changes of cardiac precursors during early heart tube formation in the presence of LPS [14].

During cardiogenesis primordial heart tube arises predominantly from splanchnic mesoderm cells, which derive from bilateral fields and merge at middle line of carcinogenic region. Spatial-temporal cardiogenesis includes primary heart tube fusion, cardiac looping and accretion, cardiac septation and coronary vasculogenesis [15].

Heart development is a very complicated process, precisely regulated by spatio-temporal gene expressions at different developmental stages. Fibroblast growth factor (FGF)-signaling is required for the migration of pro-cardiac mesoderm cells in *Drosophila* and chicks [16, 17]. Cardiac precursor cell specification occurs when the cells reach to the anterior lateral plate mesoderm. As an important inducer of myocardium, Bone morphogenetic protein 2 (BMP2) stemmed from anterior endoderm, plays an important role in heart-inducing activity of the chick embryo. Moreover, Nkx2.5, GATA factors, BMP2, myocardin, and Tbx20 are all considered to be the important cardiogenic transcription factors that characterize and induce cardiogenic differentiation [18]. Therefore, the early gastrula stage is an extremely high risk period for cardiogenesis since it is sensitive to many harmful external factors [19], which could promote the risk of congenital heart disease if there is interference with migration or differentiation of cardiac precursor cells.

In this study, the LPS levels of structural shift of the gut microbiota human and mice have been determined with the results suggesting that microbiota-derived LPS exposure inhibited embryo survival. Using chick embryos, the risk of cardiac bifida was found to be increased during embryonic cardiogenesis. Excess ROS generation might be involved in the mechanism of LPS-induced the phenotypes of cardiac bifida through affecting the vital gene expressions in heart tube formation.

Materials and methods

Experimental animals and embryos

Mice: All processes involving animal treatment in this study were in accordance with the procedures of Ethical Committee for Animal Experimentation, Jinan University. The Kunming mice used in the current study were obtained from the Laboratory Animal Centre of Sun Yat-Sen University (Guangzhou, China). All animals

were maintained under environmentally-controlled conditions, $23 \pm 2^{\circ}\text{C}$, with relative humidity of $55 \pm 10\%$, under a 12-hour light/dark cycle, with free access to standard laboratory diet and water. Five-weeks female mice were used to induce gut microbiota imbalance by injecting physiological saline (20ml/kg body weight), LPS (10 $\mu\text{g/ml}$, 20ml/kg body weight; Sigma, USA), lincomycin hydrochloride (LH, 0.3g/ml, 24ml/kg for each mouse; Shanghai Macklin Biochemical Co.,Ltd) over three consecutive days. Two female mice were housed with one normal male mouse overnight in a cage. The day that the vaginal plugs were observed was designated as embryonic day 0.5 (E0.5), whilst on E13.5 mouse embryos were harvested. All processes involving animal treatment in this study were in accordance with the procedures of Ethical Committee for Animal Experimentation, Jinan University.

Chick embryos: Fertilized chick eggs were obtained from the Avian Farm of the South China Agriculture University. The eggs were incubated until the required HH stage[20] in a humidified incubator (Yi heng Instrument, Shanghai, China) at 38°C and 70% humidity. EC (early chick) culture [21] was employed to culture these gastrula chick embryos since it met the experimental requirements. For the LPS-treated embryos, the HH0 chick embryos in EC culture were treated with either 10 $\mu\text{g/ml}$ LPS (Sigma, USA) or simple saline (control) until the experimentally-required developmental stage. For the vitamin C-treated embryos, the HH0 chick embryos in EC culture were incubated with 2.86 mM (=0.5 mg/ml) vitamin C (Beijing Ding Guo Chang Sheng, China) according with experimental requirements[22, 23]. Briefly, LPS or vitamin C was directly applied to either EC culture or *in vitro* culture medium to reach the final concentrations 10 $\mu\text{g/ml}$ (LPS) and 2.86mM vitamin C, respectively. Treated embryos were subsequently incubated for either 18 or 45 hours before being fixed with 4% paraformaldehyde for analysis of morphology and gene expression. For LPS exposure at a later embryonic stage, HH10 chick embryos were exposed 10 $\mu\text{g/ml}$ through injection into windowed eggs *in vivo* and then further incubated for 5.5 days; the surviving embryos were harvested for further assessment.

Serum collection and endotoxin determination

Whole blood samples were collected from late negative (LN) and late positive (LP) patients [24] or mice. This study was approved by the local ethics committee of The First Affiliated Hospital of Jinan University. All patients provided written informed consent. Serum was separated from the blood by centrifugation at room temperature and stored at -80°C . Serum endotoxin levels were measured according to endotoxin detection kit (Xiamen Horseshoe Crab Reagent Manufactory Co., Ltd, China) by UV spectrophotometry.

Gene transfection and tissue transplantation

HH3 chick embryos in EC culture were transfected with the GFP gene by electroporation. Briefly, 0.5 ml plasmid DNA (1.5 mg/ml GFP) was microinjected into the space between the vitelline membrane and the epiblast of HH2-3 chick embryos. Electroporation was then implemented with the electroporation parameters previously described [17]. After electroporation, the embryos were further incubated for 5 hours before the primitive streak tissues were used for transplantation. The labeled GFP⁺ primitive streak tissue was isolated from the anterior region of the primitive streak and grafted into the same position and developmental stage of an untransfected host chick embryo. Embryos were then incubated in the culture dishes of either both-side uniform sample saline or one-side containing LPS for 6 or 16 hours before being photographed (Fig. 5A).

Explant, primary and cell culture

Explant culture: HH3 chick embryo primitive streak is divided into six equal size portions, and the anterior primitive streak (cardiac progenitor cells) is deemed to be the second segment of explants from the cranial side (Fig. S4A). The explants of anterior primitive streaks were cultured *in vitro* in culture medium (DMEM-F12 GIBCO) at 37°C and 5% CO_2 [25] for 24, 48 or 72 hours. Each treatment was performed in triplicate. Approximately, 95% of the cells in the explant culture were determined to be cardiomyocytes in the control group, which shows the presence of myosin heavy chain

using MF20 immunofluorescent staining as previously reported [26].

Primary culture: Primary cardiomyocyte cultures were established from day 14 chick embryo hearts (DMEM-F12 GIBCO).

Cell culture: H9c2 cells was purchased from Guangzhou Jennio Biotech Co.,Ltd, China and cultured in culture medium (DMEM-F12 GIBCO).

Histology

Briefly, 5.5-day-old chick embryos (Control and LPS treated) were fixed in 4% paraformaldehyde at 4 °C for 24 h. The specimens were then dehydrated, cleared in xylene, and embedded in paraffin wax before being serially sectioned at 5 µm using a rotary microtome (Leica, RM2126RT, Wetzlar, Hessen, Germany). The sections were stained with hematoxylin and eosin (H&E) or immunohistochemically

In situ hybridization

Whole-mount *in situ* hybridization of chick embryos was performed according to a standard *in situ* hybridization protocol [27]. Briefly, Digoxigenin-labeled probes were synthesized for VMHC, GATA5 [22, 28], Nkx2.5 (supplied by Dr. Thomas M. Schultheiss). The whole-mount stained embryos were photographed and then frozen sections were prepared on a cryostat microtome (Leica CM1900) at a thickness of 14-18 µm.

Immunofluorescent staining and F-actin

The chick embryos were harvested after a given time incubation and fixed in 4% PFA overnight at 4°C. Whole-mount embryo immunostaining was performed using the following antibodies: MF20 (1:500, DSHB, USA), pHIS3 (*p*-histone H3, 1:400, Santa Cruz Biotechnology, USA) and C-caspase3 (Cleaved Capase-3, 1:200, Cell Signaling, USA). Briefly, the fixed embryos were then incubated with MF20, pHIS3 or C-caspase3 primary antibody at 4°C overnight on a shaker. Following extensive washing, the embryos were incubated with either anti-mouse IgG conjugated to Alexa Fluor 555 or anti-rabbit IgG conjugated to Alexa Fluor 488 overnight at 4°C on a rocker. For F-

actin detection, the cultured cells were stained using phalloidin-Alexa-Fluor 488 (1:200, Invitrogen) at room temperature for 2 hours. All the embryos were later counterstained with DAPI (1:1000, Invitrogen, USA) at room temperature for 1 hour.

Western blot

HH10 chick embryos were collected and lysed with CytoBuster™ Protein Extraction Reagent (#71009, Novagen). Total protein concentrations were assessed via a BCA quantification kit (BCA01, DingGuoBioTECH, CHN). Samples containing identical amounts of protein were fractionated by SDS-PAGE, and then transferred to PVDF membranes (Bio-Rad). Membranes were blocked with 5% Difco™ skim milk (BD) and subsequently incubated with primary and secondary antibodies, then bands of interest protein were visualized using the ECL kit (#34079, Thermo) and GeneGnome5 (SYNGENE). Gray scale of bands was analyzed using Quantity One software (Bio-Rad). Antibodies: VEGFR2 (Abcam, USA); GATA4 (Abcam, USA); TBX5 (Abcam, USA); GATA6 (Abcam, USA); PCNA (Santa Cruz Biotechnology, USA); c-Caspase3 (Cell Signaling, USA); HRP-conjugated anti-mouse IgG, HRP-conjugated anti-rabbit IgG (Cell Signaling Technology, USA). All primary antibodies were diluted 1000-fold in 5% skim milk, and secondary antibodies were diluted 2000-fold.

RNA isolation and quantitative PCR

Total RNA was isolated from HH10 chick embryos using a Trizol kit (Invitrogen, USA) according to the manufacturer's instructions. First-strand cDNA was synthesized to a final volume of 20 µl using iScript™ cDNA Synthesis Kit (BIO-RAD, USA). Following reverse transcription, PCR amplification of the cDNA was conducted as described previously [29, 30]. SYBR® Green qPCR assay were performed using a Primer Script™ RT reagent kit (Takara, Japan). All specific primers used are described in Supplementary Figure S8. Reverse transcription and amplification reactions were performed in Bio-Rad S1000™ (Bio-Rad, USA) and ABI 7000 thermal cyclers, respectively. The housekeeping gene GAPDH was run in parallel to confirm that equal

amounts of RNA were used in each reaction. The ratio between intensity of the fluorescently stained bands corresponding to genes and GAPDH was calculated to quantify the level of the transcripts for those genes mRNAs.

Fecal samples were collected from ileocecal junction; the samples were stored in a refrigerator with a temperature of -80 °C. Total 16SrRNA was isolated from mice fecal using a stool RNA kit (OMEGA BIO-TEK) according to the manufacturer's instructions. Following reverse transcription, PCR amplification of the cDNA was performed. The 16S rRNA gene was amplified with 27F and 1492R primers, *Bacillus bifidus*, *Lactobacilli* and *Escherichia coli* primers used are described in Supplementary Figure S8. The ratio between intensity of the fluorescently stained bands corresponding to genes and 16SrRNA was calculated to quantify the level of the transcripts for those genes mRNAs.

Measurement of SOD, GSH-Px and MDA

Samples from HH10 chick embryos or primary cardiomyocytes were homogenated and used for measuring the levels of SOD (superoxide dismutase), GSH-Px (glutathione peroxidase) and MDA (malondialdehyde). The protein content of the chick embryos or primary cardiomyocytes was determined using a Coomassie brilliant blue kit (Beijing Dingguo, China). The SOD, GSH and MDA activities were determined following the manufacturer's instructions (Nanjing Jiancheng, China), respectively, by UV spectrophotometry.

Photography

Following immunofluorescent staining or *in situ* hybridization, whole-mount embryos were photographed using a stereo-fluorescent microscope (Olympus MVX10) and associated Olympus software package Image-Pro Plus 7.0. The embryos were sectioned into 14 µm-thick slices using a cryostat microtome (Leica CM1900), and sections were photographed using an epi-fluorescent microscope (Olympus LX51, Leica DM 4000B) with the CN4000 FISH Olympus software package.

Data analysis

Statistical analysis for all the experimental data generated was performed using a SPSS 13.0 statistical package program for windows. The data were presented as mean \pm SE. Statistical significance were determined using paired T test, independent samples T test or one-way analysis of variance (ANOVA). $P < 0.05$ was considered to be significant.

Results

The increased the level of LPS induced by structural shift of the gut microbiota affected the reproduction ability in mouse.

In an earlier study, a significant structural shift of the gut microbiota was reported in Preeclampsia patients, which might be associated with the occurrence and development of the disease [24]. Therefore the LPS level in serum of LN and LP patients were examined, and it was found that the LPS level is increased in LP ($P > 0.05$; Fig. 1A). When the pregnant mice were treated with physiological saline and LH, which is effective against Gram-positive bacteria (Fig. 1B), quantitative real-time PCR revealed that the LH could significantly protect against *Bacillus bifidus* and *Lactobacilli*, with the result that there is more *Escherichia coli* in LH-treated mouse gut compared with their controls (Fig. 1C). LPS levels were very significantly increased in both LH- and LPS-treated mice compared with the control (control and LH: $P < 0.01$; control and LPS: $P < 0.001$; Fig. 1D). The numbers of embryos in E13.5 were observed to be lower in both LH- and LPS-treated mice compared with the control group (control and LH: $P < 0.001$; control and LPS: $P < 0.001$; Fig. 1E).

LPS exposure leads to the malformation of early Cardiogenesis of chick embryos.

Gut microbiota dysbiosis is known to generate LPS (lipopolysaccharides, endotoxin), which could penetrate the placental barrier and impact on embryo development. The effect of LPS on general development of embryos was studied using an early chick

embryo experimental model because it can be easily manipulated at the embryonic developing stage[14]. Exposure to 10µg/ml LPS at gastrula stage caused the reduction of 5.5-day chick embryo size and weight ($P < 0.05$; Figs. S1B-B1, C-C1, D-D1, E). Meanwhile, both survival rate (Fig. S1F) and developmental defect rate (Fig. S1G) of embryos at this stage increased in comparison to the control group. Two main types of phenotypes in LPS-exposed embryos were observed, a cohort of mid-defects possess relatively normal heart ventricles (Fig. S2B) compared to control (Fig. S2A), whereas in the severe defect group (Fig. S2C) the heart ventricles could not be seen. In the sections of MF20-immunofluorescent stained 5.5-day hearts (Figs. S2D-F), both the trabecula ($P < 0.001$; Fig. S2G) and ventricular wall ($P < 0.001$; Fig. S2F) were significantly thicker in LPS-induced heart mid-defect group than in controls (Figs. S2D1-D2, E1-E2, F1-F2).

An investigation into whether LPS-induced abnormal cardiogenesis occurred in the stage of heart tube formation was carried out using early gastrula chick embryos (Fig. 2), so that whole-mount MF20 immunofluorescent staining were implemented on the HH10 chick embryos to determine the heart tube formation chick embryos in presence/absence of LPS. It is evident that the left C-looping heart tube has been formed in control embryos (Figs. 2B-B1), while three kinds of phenotypes [including right looping (Figs. 2C-C1), hypertrophy (Figs. 2D-D1) and cardiac bifida (Figs. 2E-E1)] were present in differing proportions (Fig. 2F) in LPS-treated groups. This observation was confirmed by the transverse sections of MF20 immunofluorescent stained control and LPS-induced cardiac bifida (Figs. 2G-J), in which the bifida of heart tube in LPS-treated embryos could be clearly seen (Figs. 2J1-J2) whilst the heart tube remains intact in control embryos (Figs. 2H1-H2). A similar experimental finding resulted in whole-mount VMHC *in situ* hybridization (Figs. 2K-L) and their corresponding transverse sections (Figs. 2L-N). All these data indicate that LPS exposure in early gestation indeed could cause malformation of early chick embryo hearts.

LPS exposure restricted the cell migration of cardiac precursors during gastrula chick embryo development.

Using a combination of GFP transfection with anterior primitive streak allograft, shown in Fig. 3A, the GFP⁺ cardiac progenitor cell migration was examined in the presence/absence of LPS in EC culture medium. To avoid the diversity of embryo developmental velocities, gastrula chick embryos were employed in home-made 35mm-diameter culture dishes in which a barrier blocks the medium flow between both sides (Fig. 3A). The embryos with the allograft of GFP⁺ anterior primitive streaks were photographed with fluorescence and bright-field after 0-, 5- and 16-hour incubations, respectively. The results showed that GFP⁺ cardiac progenitor cells evenly migrate toward to the site of primary heart field in controls (Figs. 3B-D, B1-D1); whilst in the LPS- exposed half-side embryos, many fewer GFP⁺ progenitor cells migrate forward in comparison to the saline sample control (Figs. 3E-G, E1-G1). F-actin immunofluorescent staining images indicated that fewer cell protrusions were generated in the setting of LPS (Figs. 3, H-K, I1, K1), which is reflected by the ratios of cell long axis/short axis ($P < 0.01$; Fig. 3L) and cellular stress fibers ($P < 0.01$; Fig. 3M).

In addition, DiI was micro-injected into anterior primitive streak of HH4 gastrula chick embryos, and DiI labeled cardiac progenitor cell migration was studied in the presence/absence of LPS using the above-mentioned strategy (Fig. S3A). Two parallel cell migration trajectories of the DiI⁺ cardiac progenitor cells were found after 15-hour incubation in control embryos (Figs. S3B-D, B1-D1); but very few DiI⁺ cardiac progenitor cells could be seen in the LPS-exposed side of embryo compared to their controls (Figs. S3E-G, E1-G1).

To confirm the *in vivo* results, explant cultures of anterior primitive streak (Figs. S4B-B2, C-C2) and H9c2 cell cultures (Figs. S4E-E2, F-F2) were studied *in vitro* in the presence of LPS. After 24- and 48-hour incubations, areas of the cell extensions sent forth from the explants of anterior primitive streaks *in vitro* culture were measured, and it could be demonstrated that fewer cell extensions occurred in the presence of LPS than in controls (Fig. S4D). Moreover, in “scratch wound” migration assays of H9c2 (a

permanent cell line derived from rat cardiac tissue) cells, the “gap closure” was shown to be much slower in LPS-treated cells than in untreated controls, based on the photographs after 12- and 24-hour incubations ($P < 0.001$; Figs. S4G). Taken together, this is suggestive that LPS exposure at gastrula chick embryo indeed could repress the cell migration of cardiac progenitor cells toward to primary heart field.

LPS exposure influenced the differentiation of cardiac precursors during gastrula chick embryo development.

The gene expressions related to heart tube formation were determined in presence of LPS by whole-mount *in situ* hybridization, immunofluorescent staining, western blot and quantitative PCR (Fig.4). The GATA5 and Nkx2.5 whole-mount *in situ* hybridization showed that both GATA5 and Nkx2.5 expressions in the LPS-treated side of embryos were dramatically reduced in comparison to opposite control sides (Figs. 4A-A1, B-B1), which could also be clearly seen in their transverse sections (Figs. 4A1'-B1'). Using MF20 immunofluorescent staining, fewer MF20⁺ cells were evident in the monolayer cells emanating from the *in vitro* cultured explant of anterior primitive streak in LPS-treated group compared to control (Figs. 4D-D1, E-E1). Western blotting was employed to determine the expressions of early heart tube formation relevant genes in HH10 chick embryos exposed to LPS, and demonstrated that the expressions of VEGFR2 ($p < 0.01$) and TBX5 ($p < 0.001$) were up-regulated to some extent while GATA6 ($p < 0.001$) was down-regulated by LPS exposure. No change was found in GATA4 (Figs. 4G-G1). Moreover, quantitative PCR data showed more gene expression alterations induced by LPS exposure, which are the down-regulated Nkx2.5, BMP2, GATA5, VMHC and up-regulated TBX20 in both HH7 and HH10 chick embryos exposed to LPS; while Nkx2.6 were down-regulated and TBX20 were up-regulated in HH10 chick embryos. No change was seen in GATA4 expression reduced at mRNA level in HH10 chick embryos exposed to LPS (Figs. 4C, F). These data imply that LPS exposure certainly altered crucial gene expressions for heart tube formation during early embryo development which, in turn, interfere with the differentiation of cardiac

progenitor cells.

LPS exposure suppressed cell proliferation and enhanced cell apoptosis during gastrula chick embryo development.

The LPS-induced reduction of cardiac progenitor cells could also be due to the inhibition of *in vivo* cell proliferation and apoptosis following the exposure to LPS. Whole-mount co-immunofluorescent staining of MF20 and pHIS3 was carried out in gastrula chick embryos exposed to simple saline (control, Figs. 5A, C) and LPS (Figs. 5B, D). The assessment of pHIS3⁺ cell numbers in MF20⁺ heart tube sections showed that there were less pHIS3⁺ cells in LPS-treated heart tubes than in controls ($P < 0.01$; Figs. 5C1-C3, D1-D3, E). Meanwhile, western blot data showed that PCNA expression at the protein level was also significantly down-regulated in the LPS-treated group ($P < 0.001$; Figs. 5K, L). Furthermore, immunofluorescent staining against pHIS3 was implemented on the *in vitro* cultured H9c2 cells, and showed the similar tendency, with less pHIS3⁺ cells being found in LPS-treated group compared to the control groups ($P < 0.01$; Figs. S5A-A2, B-B2, C).

The whole-mount co-immunofluorescent staining of MF20 and C-caspase3 in gastrula chick embryos was implemented to detect cell apoptosis in the heart tubes exposed to LPS (Figs. 5F-I). Counting C-caspase3⁺ cells on their corresponding transverse sections of heart tubes showed that there were more c-Caspase3⁺ cells in LPS-treated group than in controls ($P < 0.01$; Figs. 5H1-H3, I1-I3, J). This was confirmed by western blot data about C-caspase3 protein expression in HH10 chick embryos ($P < 0.001$; Fig. 5M, N). Likewise, more PI (propidium iodide)-positive cells were evident in LPS-treated H9c2 *in vitro* cultured cells than in controls ($P < 0.001$; Figs. S5D-D2, E-E2, F). It is suggested that LPS exposure is able to suppress proliferation and promote apoptosis of cardiac progenitor cells.

The excessive ROS is responsible for LPS exposure-induced malformation of heart tubes during gastrula chick embryo development.

Superoxide dismutase (SOD), glutathione (GSH) and malondialdehyde (MDA) activity assay kits were used to determine the activities of SOD, GSH and MDA in HH10 chick embryos exposed to either simple saline (control) or LPS (Figs. 6A-C). The results showed that SOD activity reduced in presence of LPS ($P < 0.05$; Fig. 6A). The activities of both GSH (control and LPS: $P < 0.01$; LPS and LPS + vitamin C: $P < 0.05$) and MDA (control and LPS: $P < 0.001$; LPS and LPS + vitamin C: $P < 0.001$) increased in the presence of LPS but fell back again after addition of vitamin C (Figs. 6B-C). The quantitative PCR data showed that the expressions of SOD1, SOD2 and GPX at the mRNA level were up-regulated by LPS treatment, but addition of vitamin C again showed a normalizing effect (Fig. 6D). This adverse effect of vitamin C against LPS-induced abnormality was also seen in MF20 immunofluorescent-stained heart tube formation, which appeared to be normal as control (Figs. 6E-H, G1-G2, H1-H2) and abnormality rate dramatically decreased following addition of vitamin C (Fig. 6I). Furthermore, the expressions of the key genes related to heart tube formation were determined and showed that LPS-exposure led to the expression reduction of VMHC, GATA5, BMP2, Nkx2.5, TBX5, Mmp2, Epha3, Epha1 and Tmem2 in HH10 chick embryos exposed to LPS, but that all of their expressions were recovered to some degree after addition of vitamin C (Fig. 6J).

Next, photographs (Figs. S6A-C) and determinations of ROS activity (Fig. S6D) were taken after 24-hour incubations in the primary culture of chick cardiac muscle cells exposed to the combined application of $228\mu\text{M}$ ($=40\mu\text{g/ml}$) vitamin C and $10\mu\text{g/ml}$ LPS. The result showed that LPS exposure induced the increase of ROS activity but showed a significant drop when the after application of vitamin C and LPS together (control and LPS: $P < 0.001$; LPS and LPS + vitamin C: $P < 0.001$; Fig. S6D). In addition, when $228\mu\text{M}$ vitamin C was added into the cultured H9c2 cells in presence of LPS, LPS treatment allowed the reduction of pHIS3⁺ cell numbers to recover to some extent (control and LPS: $P < 0.01$; Figs. S6E-N).

All these data showed that LPS could promote the cell apoptosis of cardiac

progenitor cells. Here, using flow cytometry, it has been demonstrated that LPS-exposure increased cell apoptosis, but application of vitamin C and LPS together distinctly suppressed the increase of LPS-induced cell apoptosis in the cultured chick cardiac muscle cells (control and LPS: $P < 0.001$; LPS and LPS + vitamin C: $P < 0.001$; Figs. S7A-D). Similar experiments were carried out with cultured H9c2 cells immunofluorescent stained with PI, the results also showing that the combinations of vitamin C and LPS obviously repressed the increase of LPS-induced PI⁺ H9c2 cells (control and LPS: $P < 0.001$; LPS and LPS + vitamin C: $P < 0.001$; Figs. S7E-N). Vitamin C, as an anti-oxidant, could reduce the various LPS-induced the alterations of cell proliferation and apoptosis, further indicating that excessive ROS production might elevate the percentage of abnormal heart tube formation induced by LPS exposure.

Discussion

It has been known that while many congenital diseases are induced by external environmental harmful factors, such as folate deficiency and teratogens, exposure in the first weeks of human gestation may cause severe congenital heart defects [31]. However, since most pregnancies are not planned, people might not undertake any precautionary protective actions until they are sure about their pregnancies. The reason that birth defects occur frequently in nervous and cardiovascular systems is because they develop at the earliest stage of embryogenesis. Maternal LPS could come from intestinal microbiota imbalance or from the infection of pregnant women at various stages of gestation. It has been confirmed in this work that the high level of LPS occurs in LP patients (Fig. 1A) when data from the mouse model revealed the relationship between intestinal microbiota imbalance and embryonic survival rate. When mice were treated with LH, the LPS level was increased and embryonic survival rate decreased (Figs. 1B-E). All the above results suggested the possibility that LPS could be a potential teratogen in both human and mouse. LPS directly applied to pregnant mice yielded the similar phenotype which led to investigation of the potential mechanism by which LPS affects survival of embryos. LPS exposure will enhance the risk of embryonic heart malformation for the affected offspring, as shown by *in vitro*

experiments of embryonic cardiomyocytes [32]. Once the mechanism of LPS-induced cardiac birth defects is understood, rational precautionary measures could be effectively implemented.

In this study, avian models are employed because of the advantages they offer for extrapolating the effect of LPS on embryo development to human pregnancy. Using early gastrulating chick model, LPS exposure at gastrula stage was found to significantly reduce embryo weight and cause the death and abnormal developments of some embryos (Figs. S1, S2). Meanwhile, LPS also increased the incidence of chick heart tube malformations, including right looping, hypertrophy and cardiac bifida, which was clearly displayed by MF20- and VMHC- labeled heart tube in whole-mount and transverse sections (Fig. 2). Bladet *al.* reported that preterm lambs were more sensitive to LPS exposure than were more mature foetuses in terms of myocardial/cardiovascular responses (electrocardiography and heart rate) [33], suggesting that foetal cardiac functions could also be impacted by LPS exposure. The mechanism of LPS exposure-induced malformation of heart tubes could be complex. It is well known that cardiac precursors in first heart field derive from anterior primitive streak cells of gastrulating embryos. These cardiac precursors migrate toward to the site of heart tube formation, which is assuredly an essential initial step for normal heart tube formation [17]. Using *in vivo* allograft or Dil labeling of anterior primitive streaks of gastrula chick embryos in presence of LPS, it was demonstrated that LPS exposure could significantly inhibit the migratory ability of cardiac precursors toward the first heart field (Figs. 3, S3). The reduction of cardiac precursor migratory ability was also confirmed by the following observations: 1) fewer cells emigrated from *in vitro* cultured anterior primitive streak explants, 2) decreasing healing velocity in wound scratch assay of H9c2 cells in the setting of LPS (Fig. S4). Similar experimental data indicated that the migratory ability of cardiac precursor cells was negatively influenced in gastrula chick embryos exposed to LPS.

The morphogenesis of heart tubes depends on normal spatiotemporal gene expressions of cardiomyocyte differentiation relevance such as GATA5 and Nkx2.5 etc[34]. Whole-mount *in situ* hybridization and immunofluorescent staining showed

that LPS exposure dramatically restricted the expression of GATA5 and Nkx2.5 at cardiac crescent and of MF20 in extended cells from *in vitro* cultured anterior primitive streaks (Fig. 4). Not only these genes, but also the expressions of VEGFR2, GATA4, TbX5, GATA6 etc., were disturbed by LPS exposure at early gastrula stage of embryos (Fig. 4). As zinc-finger transcription factors, the GATA family perform vital functions in heart formation since bilateral heart tubes (cardia bifida) and fewer cardiomyocytes could occur in GATA4 knock-out mice. GATA4, GATA5 deficiencies also leads to cardia bifida, while the over-expression of GATA5 results in ectopic Nkx2.5 expression with ectopic beating cells in fish embryos [18]. Both the published literature and the results of the work reported here indicate that LPS induces the disorder of crucial gene expressions on controlling cardiomyocyte differentiation during heart tube formation. This could then partially contribute to the above-mentioned phenotypes.

Van den Berg *et al.* reported that there are proliferating growth centers in the caudal coelomic walls, and that these play an important role on elongating the heart tube and provide structural support for early heart formation [35]. In this study, using embryonic heart tube and primary cardiomyocytes, cell proliferation in cardiac progenitor cells were demonstrated to be inhibited by LPS exposure (Figs. 5, S5). Ghatpandeet *al.* found that either addition of retinoic acid or anterior endoderm transplantation is able to reduced cell apoptosis and GATA4 expression, which maintains normal heart tube morphogenesis [36], suggesting the importance of cell apoptosis during cardiogenesis. Both the results of *in vivo* and *in vitro* studies described here indicate that cell apoptosis of cardiac precursors are raised following the exposure to LPS during gestation (Figs. 5, S5), which would be associated with subsequent heart tube malformation.

Earlier work revealed that many external factors, including high glucose and ethanol, could be hazardous factors in causing malformation of embryonic heart tube [26, 37], in which excessive ROS generation was observed, thereby implying that ROS plays a vital role in the pathological process. In this study, LPS exposure was observed to reduce the activities of SOD and increase the activities of GSH and MDA in embryo heart tubes and primary culture of chick cardiomyocytes (Fig. 6). The combination of vitamin C and LPS could to an extent reduced LPS-induced apoptosis increase and

proliferation reduction implying that excessive ROS production mediated LPS exposure-induced malformation of heart tubes(Figs. S6-7).

In other words, excess production of O₂ radicals induced by LPS exposure could, in turn, initiate cell apoptosis in embryonic cells, and so, impair normal embryo development. This is similar to the discoveries of ethanol-induced embryonic dysplasia through stimulating ROS generation [38-40]. In LPS-induced adult diseases, accumulating evidence suggests that ROS play an important role in cardiac- and hepatic dysfunctions during various inflammasomes and endotoxemia [41, 42].

In summary, it has been demonstrated that LPS was induced in gut microbiota imbalance in mice, and observed that LPS exposure during early chick embryo development increased the risk of various malformations of heart tubes including cardia bifida. LPS exposure at gastrula stage can inhibit cell proliferation and enhance cell apoptosis of cardiac precursors. In the context of LPS, excessive ROS is produced during heart tube formation, and both cell migration and differentiation-related gene expressions (Nkx2.5 and GATA5 etc.) of cardiac progenitor cells were interfered with. As a consequence, the malformation of heart tube such as cardia bifida resulted, which is schematically summarized in Fig. 7. There is no doubt that studies in this field illuminate the opportunities for congenital heart disease prevention and treatment. However, further experimentation is needed to explore the precise molecular biological mechanisms.

Acknowledgements

This study was supported by NSFC grant (31771331, 81571436, 31401230), Science and Technology Planning Project of Guangdong Province (2014A020221091, 2017A020214015, 2016B030229002, 2014A020213008, 2017A050506029), Science and Technology Program of Guangzhou (201710010054, 201510010073), Guangdong Natural Science Foundation (2016A030311044), The Fundamental Research Funds for the Central Universities (21617466) and Research Grant of Key Laboratory of Regenerative Medicine, Ministry of Education, Jinan University (No. ZSYX-M-00001

Conflict of interest

The authors declare that they have no conflict of interest.

Figure legends

Figure 1. The relationship of LPS level induced by the structural shift of the gut microbiota and survival of mouse embryos.

A: Mean plasma LPS values (EU/ml) from the LN and LP. **B:** The sketches illustrate pregnant mice treated with physiological saline (control), LH and LPS and then harvested on E13.5. **C:** Quantitative real-time PCR was used to measure fecal bacterial DNA (*Bacillus bifidus*, *Lactobacilli* and *Escherichia coli*) in ileocecal junction of the mouse embryos. **D:** Mean plasma LPS values (EU/ml) for all assay results from the control, LH and LPS treated mice. **E:** The number of mouse embryos in the control, LH and LPS treated mice. Abbreviation: **LPS:** Lipopolysaccharides; **LN** (Late Negative): third trimesters without Preeclampsia; **LP** (Late Positive): third trimesters with Preeclampsia; **LH:** Lincomycin hydrochloride.

Figure 2. The heart tube formation of early chick embryo following LPS exposure.

A: The sketches illustrate early chick embryos treated with 10µg/ml LPS and harvested at HH10. **B-E, B1-E1:** The representative whole-mount MF20 immunofluorescent images of heart tubes from control (B) and LPS-treated (C-E) chick embryos, respectively. B1-E1 schematically illustrate the appearance of heart tubes in B-E, respectively. **F:** The bar chart showing the percent distribution of various heart tube phenotypes between control and LPS groups. **G-H:** The representative bright-field images of HH10 chick embryos from control (G) and LPS-treated (H) groups, respectively. **I-J:** The representative MF20 immunofluorescent images of heart tubes of HH10 chick embryo from control (I) and LPS-treated cardiac bifida (J) groups,

respectively. **I1-J1, I2-J2**: The transverse sections were taken at the levels indicated by dotted lines in I-J, respectively. I2-J2 are merged images of I1-J1 and DAPI staining. **K-L**: The whole-mount VMHC *in situ* hybridization images of heart tubes from control (K) and LPS-treated cardiac bifida (L) groups, respectively. **M-N**: The transverse sections were taken at the levels indicated by dotted lines in K-L, respectively. Scale bars = 20 μm in B-E, 50 μm in G,I, 10 μm in H, J, K, M and 30 μm in H1-H2, J1-J2, L, N.

Figure 3. LPS restricts GFP-labeled anterior primitive streak cell migration during gastrula chick embryo development.

A: The sketches illustrate the combination of GFP electroporation and graft implantation with the exposure to LPS (see material and method in detail). **B-D, B1-D1**: The fluorescent images were taken at 0h (B), 6h (C) and 16h (D) after GFP-labelled anterior primitive streak was allografted in the control embryo. B1-D1 are merged images of B-D and bright-field images, respectively. **E-G, E1-G1**: The fluorescent images were taken at 0h (E), 6h (F) and 16h (G) after GFP-labelled anterior primitive streak was allografted in the embryo exposed to LPS at half-side. E1-G1 are merged images of E-G and bright-field images, respectively. **H-K, I1, K1**: The representative F-actin fluorescent staining images were taken from control (H-I) and LPS-treated (J-K) groups. I1 and K1 are the high magnification images taken from the sites indicated by dotted line squares in I-K, respectively. **L**: The bar chart compares the ratios of F-actin-stained cell long axis and short axis between control and LPS groups. **M**: The bar chart compares F-actin-stained intracellular fibers between control and LPS groups. Scale bars = 50 μm in B-G, B1-G1, 20 μm in H-K, 100 μm in I1, K1.

Figure 4. Determining gene expressions related to cardiac progenitor cell differentiation following LPS treatment.

A-B: The GATA5, Nkx2.5 *in situ* hybridization was carried out on the whole-mount embryos exposed to PBS (control) or LPS. **C**: The quantitative PCR data

showing the expressions of Nkx2.5, BMP2, GATA5, VMHC and TBX20 in control and LPS-treated HH7 chick embryos. **D-D1**: The DAPI + MF20 immunofluorescent images were taken after anterior primitive streak tissue was incubated for 48 hours (D) and 72 hours (D1) in the control group. **E-E1**: The DAPI + MF20 immunofluorescent images were taken after anterior primitive streak tissue was incubated for 48 hours (E) and 72 hours (E1) in LPS-treated groups. **F**: The quantitative PCR data showing the expressions of VMHC, GATA5, BMP2, Nkx2.5, Nkx2.6, GATA4, TBX20 and TBX5 in control and LPS-treated HH10 chick embryos. **G-G1**: The western blot data (F) showing the expressions of VEGFR2, GATA4, TBX5 and GATA6 in control and LPS-treated group. F1 is the quantitative analysis for the expressions of above genes through the ratios of arbitrary unit normalized to β -actin. Scale bars = 100 μ m in A,B, 50 μ m in A1,B1, A1', B1', 20 μ m D-D1, E-E1.

Figure 5. Determining cell proliferation and cell apoptosis in heart tubes

A-B: The representative bright-field images of HH10 chick embryos from control (A) and LPS-treated (B) groups, respectively. **C-D**: The representative double immunofluorescent images of MF20 and pHIS3 at cranial regions of chick embryos from control (C) and LPS-treated (D) groups, respectively. **C1-D1, C2-D2, C3-D3**: The pHIS3-stained transverse sections (C1-D1) and DAPI-stained (C2-D2) from the levels indicated by dotted lines in C-D, respectively. C3-D3 are the images of MF20/pHIS3/DAPI staining. **E**: The bar charts compare pHIS3⁺ cell numbers in heart tubes between control and LPS group. **L-M**: The western blot data showing the expressions of PCNA in control and LPS-treated group. The lower bar chart indicates the quantitative analysis of PCNA expression through the ratios of arbitrary unit normalized to β -actin. **F-G**: The representative bright-field images of HH10 chick embryos from control (F) and LPS-treated (G) groups, respectively. **H-I**: The representative double immunofluorescent images of MF20 and C-caspases3 at cranial regions of chick embryos from control (H) and LPS-treated (I) groups, respectively. **H1-I1, H2-I2, H3-I3**: The C-caspase3-stained transverse sections (H1-I1) and DAPI-stained (H2-I2) from the levels indicated by dotted lines in H-I, respectively. H3-I3 are

the MF20/DAPI/C-caspase3 staining. **J**: The bar chart compares C-caspase3⁺ cell numbers in heart tubes in control and LPS groups. **N-O**: The western blot data showing the expressions of C-caspase3 in control and LPS-treated groups. The lower bar chart showing the quantitative analysis of C-caspase3 expression through the ratios of arbitrary unit normalized to β -actin. Scale bars = 500 μ m in A-B, F-G; 200 μ m in C-D, H-I; 50 μ m in C1-C3, D1-D3, H1-H3, I1-I3.

Figure 6. Determination of oxidative stress parameters in embryonic heart tubes in presence of LPS.

A-C: The activities of SOD (A), GSH (B) and MDA (C) in embryonic heart tubes assessed in presence/absence of LPS and vitamin C (Vc) with the determination kits. **D**: The quantitative PCR data showing the expressions of SOD1, SOD2 and GPX in control, LPS-treated and LPS + vitamin C-treated HH10 chick embryos. **E-F**: The representative bright-field images of HH10 chick embryos from the LPS + vitamin C-treated group. **G-H**: The representative MF20 immunofluorescent images of heart tubes of HH10 chick embryo from LPS + vitamin C-treated group. **G1-H1**, **G2-H2**: The transverse sections were taken at the levels indicated by dotted lines in G-H, respectively. G2-H2 are the merge images of G1-H1 and DAPI staining. **I**: The bar chart showing the percent distribution of various heart tube phenotypes between control, LPS and LPS + vitamin C groups. **J**: The quantitative PCR data shows the expressions of VMHC, GATA5, BMP2, Nkx2.5, TBX5, Mmp2, Epha3 and Tmem2 in control, LPS-treated and LPS + vitamin C-treated HH10 chick embryos. Scale bars = 500 μ m in E-G; 200 μ m in G-H and 50 μ m in G1-H1, G2-H2.

Figure 7. Model depicting the hypothesis for LPS-induced abnormalities during heart tube formation.

References

1. Hay A J, Zhu J. 2016. In sickness and in health: The relationships between bacteria and bile in the human gut. *Adv Appl Microbiol.*96:43-64.
2. Zhang Y J, Li S, Gan R Y, Zhou T, Xu D P, Li H B. 2015. Impacts of gut bacteria on human health and diseases. *Int J Mol Sci.*16:7493-7519.
3. Yang Y, Jobin C. 2014. Microbial imbalance and intestinal pathologies: Connections and contributions. *Dis Model Mech.*7:1131-1142.
4. Trajkovski M, Wollheim C B. 2016. Physiology: Microbial signals to the brain control weight. *Nature.*534:185-187.
5. Sommer F, Backhed F. 2013. The gut microbiota--masters of host development and physiology. *Nat Rev Microbiol.*11:227-238.
6. Perry R J, Peng L, Barry N A, Cline G W, Zhang D, Cardone R L, Petersen K F, Kibbey R G, Goodman A L, Shulman G I. 2016. Acetate mediates a microbiome-brain-beta-cell axis to promote metabolic syndrome. *Nature.*534:213-217.
7. Gregory K E, Samuel B S, Houghteling P, Shan G, Ausubel F M, Sadreyev R I, Walker W A. 2016. Influence of maternal breast milk ingestion on acquisition of the intestinal microbiome in preterm infants. *Microbiome.*4:68.
8. Alexander C, Rietschel E T. 2001. Bacterial lipopolysaccharides and innate immunity. *J Endotoxin Res.*7:167-202.
9. Raetz C R, Whitfield C. 2002. Lipopolysaccharide endotoxins. *Annu Rev Biochem.*71:635-700.
10. Zhao K, Song X, Huang Y, Yao J, Zhou M, Li Z, You Q, Guo Q, Lu N. 2014. Wogonin inhibits lps-induced tumor angiogenesis via suppressing pi3k/akt/nf-kappab signaling. *Eur J Pharmacol.*737:57-69.
11. Aisemberg J, Vercelli C A, Bariani M V, Billi S C, Wolfson M L, Franchi A M. 2013. Progesterone is essential for protecting against lps-induced pregnancy loss. Lif as a potential mediator of the anti-inflammatory effect of progesterone. *PLoS One.*8:e56161.
12. Straley M E, Togher K L, Nolan A M, Kenny L C, O'keeffe G W. 2014. Lps alters placental inflammatory and endocrine mediators and inhibits fetal neurite growth in affected offspring during late gestation. *Placenta.*35:533-538.
13. Wang H, Yang L L, Hu Y F, Wang B W, Huang Y Y, Zhang C, Chen Y H, Xu D X. 2014. Maternal lps exposure during pregnancy impairs testicular development, steroidogenesis and spermatogenesis in male offspring. *PLoS One.*9:e106786.
14. Rashidi H, Sottile V. 2009. The chick embryo: Hatching a model for contemporary biomedical research. *Bioessays.*31:459-465.
15. Martinsen B J. 2005. Reference guide to the stages of chick heart embryology. *Dev Dyn.*233:1217-1237.
16. Beiman M, Shilo B Z, Volk T. 1996. Heartless, a drosophila fgf receptor homolog, is essential for cell migration and establishment of several mesodermal lineages. *Genes Dev.*10:2993-3002.
17. Yang X, Dormann D, Munsterberg A E, Weijer C J. 2002. Cell movement patterns during gastrulation in the chick are controlled by positive and negative chemotaxis mediated by fgf4 and fgf8. *Dev Cell.*3:425-437.
18. Brand T. 2003. Heart development: Molecular insights into cardiac specification and

early morphogenesis. *Dev Biol.*258:1-19.

19.Daft P A, Johnston M C,Sulik K K. 1986. Abnormal heart and great vessel development following acute ethanol exposure in mice. *Teratology.*33:93-104.

20.Hamburger V,Hamilton H L. 1992. A series of normal stages in the development of the chick embryo. 1951. *Dev Dyn.*195:231-272.

21.Chapman S C, Collignon J, Schoenwolf G C,Lumsden A. 2001. Improved method for chick whole-embryo culture using a filter paper carrier. *Dev Dyn.*220:284-289.

22.Li Y, Wang X Y, Zhang Z L, Cheng X, Li X D, Chuai M, Lee K K, Kurihara H,Yang X. 2014. Excess ros induced by aaph causes myocardial hypertrophy in the developing chick embryo. *Int J Cardiol.*176:62-73.

23.Wang G, Zhang N, Wei Y F, Jin Y M, Zhang S Y, Cheng X, Ma Z L, Zhao S Z, Chen Y P, Chuai M, Hoher B,Yang X. 2015. The impact of high-salt exposure on cardiovascular development in the early chick embryo. *J Exp Biol.*218:3468-3477.

24.Liu J, Yang H, Yin Z, Jiang X, Zhong H, Qiu D, Zhu F,Li R. 2017. Remodeling of the gut microbiota and structural shifts in preeclampsia patients in south china. *Eur J Clin Microbiol Infect Dis.*36:713-719.

25.Wang X Y, Li Y, Ma Z L, Wang L J, Chuai M, Munsterberg A, Geng J G,Yang X. Retention of stem cell plasticity in avian primitive streak cells and the effects of local microenvironment. *Anat Rec (Hoboken).*296:533-543.

26.Li S, Wang G, Gao L R, Lu W H, Wang X Y, Chuai M, Lee K K, Cao L,Yang X. 2015. Autophagy is involved in ethanol-induced cardia bifida during chick cardiogenesis. *Cell Cycle.*14:3306-3317.

27.Henrique D, Adam J, Myat A, Chitnis A, Lewis J,Ish-Horowicz D. 1995. Expression of a delta homologue in prospective neurons in the chick. *Nature.*375:787-790.

28.Kamei C N, Kempf H, Yelin R, Daoud G, James R G, Lassar A B, Tabin C J,Schultheiss T M. 2011. Promotion of avian endothelial cell differentiation by gata transcription factors. *Dev Biol.*353:29-37.

29.Maroto M, Reshef R, Munsterberg A E, Koester S, Goulding M,Lassar A B. 1997. Ectopic pax-3 activates myod and myf-5 expression in embryonic mesoderm and neural tissue. *Cell.*89:139-148.

30.Dugaiczky A, Haron J A, Stone E M, Dennison O E, Rothblum K N,Schwartz R J. 1983. Cloning and sequencing of a deoxyribonucleic acid copy of glyceraldehyde-3-phosphate dehydrogenase messenger ribonucleic acid isolated from chicken muscle. *Biochemistry.*22:1605-1613.

31.Linask K K. The heart-placenta axis in the first month of pregnancy: Induction and prevention of cardiovascular birth defects. *J Pregnancy.*2013:320413.

32.Panaro M A, Acquafredda A, Cavallo P, Cianciulli A, Saponaro C,Mitolo V. 2010. Inflammatory responses in embryonal cardiomyocytes exposed to lps challenge: An in vitro model of deciphering the effects of lps on the heart. *Curr Pharm Des.*16:754-765.

33.Blad S, Welin A K, Kjellmer I, Rosen K G,Mallard C. 2008. Ecg and heart rate variability changes in preterm and near-term fetal lamb following lps exposure. *Reprod Sci.*15:572-583.

34.Wei D, Bao H, Zhou N, Zheng G F, Liu X Y,Yang Y Q. Gata5 loss-of-function mutation responsible for the congenital ventriculoseptal defect. *Pediatr Cardiol.*34:504-

35. Van Den Berg G, Abu-Issa R, De Boer B A, Hutson M R, De Boer P A, Soufan A T, Ruijter J M, Kirby M L, Van Den Hoff M J, Moorman A F. 2009. A caudal proliferating growth center contributes to both poles of the forming heart tube. *Circ Res.*104:179-188.

36. Ghatpande S, Ghatpande A, Zile M, Evans T. 2000. Anterior endoderm is sufficient to rescue foregut apoptosis and heart tube morphogenesis in an embryo lacking retinoic acid. *Dev Biol.*219:59-70.

37. Wang G, Huang W Q, Cui S D, Li S, Wang X Y, Li Y, Chuai M, Cao L, Li J C, Lu D X, Yang X. 2015. Autophagy is involved in high glucose-induced heart tube malformation. *Cell Cycle.*14:772-783.

38. Gonzalez A, Pariente J A, Salido G M. 2007. Ethanol stimulates ros generation by mitochondria through ca^{2+} mobilization and increases gfap content in rat hippocampal astrocytes. *Brain Res.*1178:28-37.

39. Bailey S M, Cunningham C C. 1998. Acute and chronic ethanol increases reactive oxygen species generation and decreases viability in fresh, isolated rat hepatocytes. *Hepatology.*28:1318-1326.

40. Brown S D, Brown L A. 2012. Ethanol (etoh)-induced tgf-beta1 and reactive oxygen species production are necessary for etoh-induced alveolar macrophage dysfunction and induction of alternative activation. *Alcohol Clin Exp Res.*36:1952-1962.

41. Yu X, Lan P, Hou X, Han Q, Lu N, Li T, Jiao C, Zhang J, Zhang C, Tian Z. 2016. Hbv inhibits lps-induced nlrp3 inflammasome activation and il-1beta production via suppressing the nf-kappab pathway and ros production. *J Hepatol.*

42. Zhao H, Zhang M, Zhou F, Cao W, Bi L, Xie Y, Yang Q, Wang S. 2016. Cinnamaldehyde ameliorates lps-induced cardiac dysfunction via tlr4-nox4 pathway: The regulation of autophagy and ros production. *J Mol Cell Cardiol.*101:11-24.

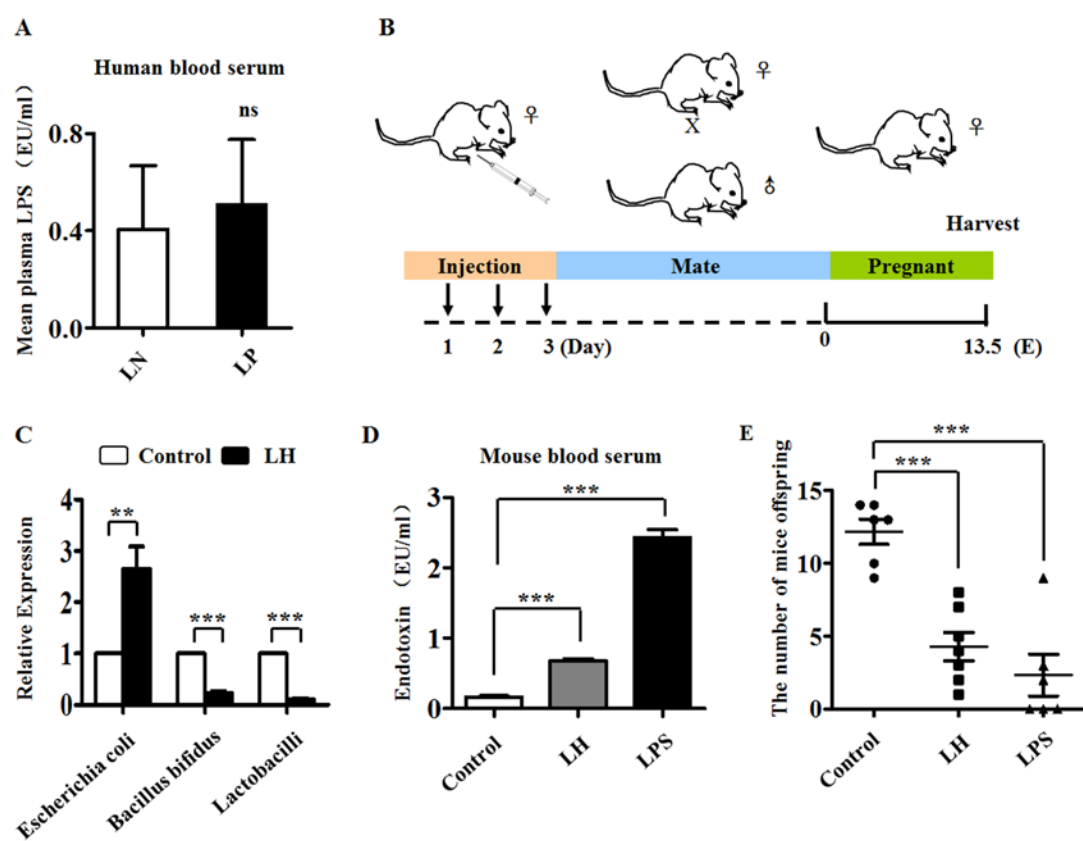


Figure 1

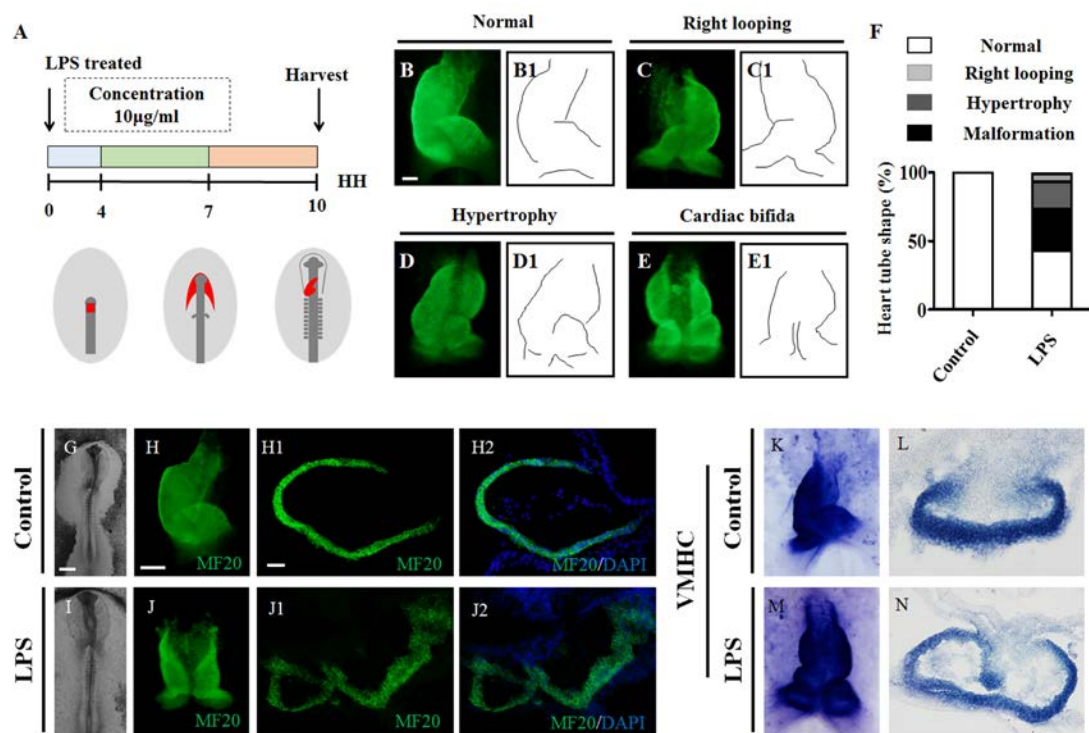


Figure 2

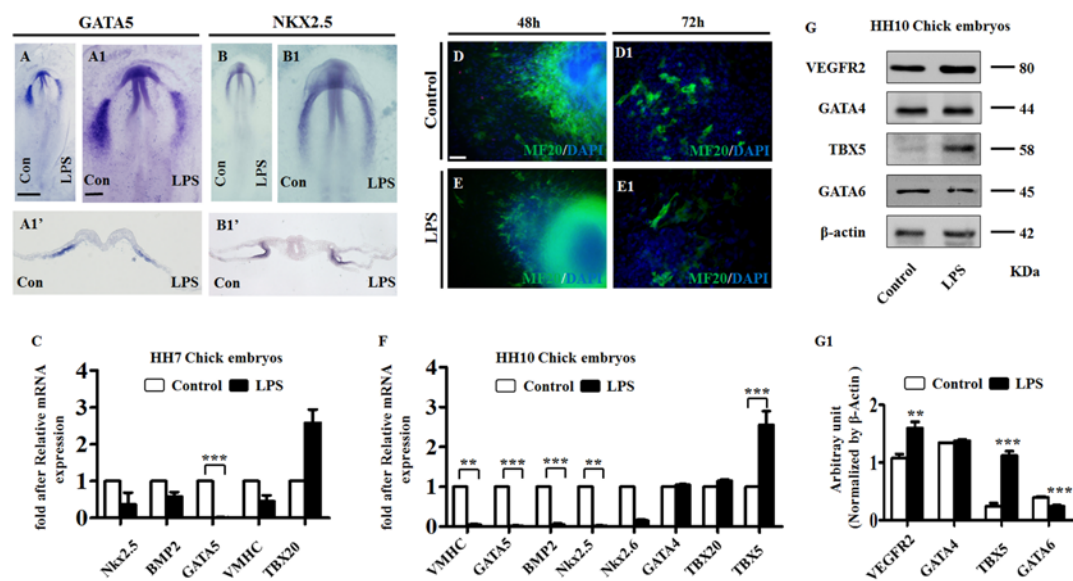


Figure 4

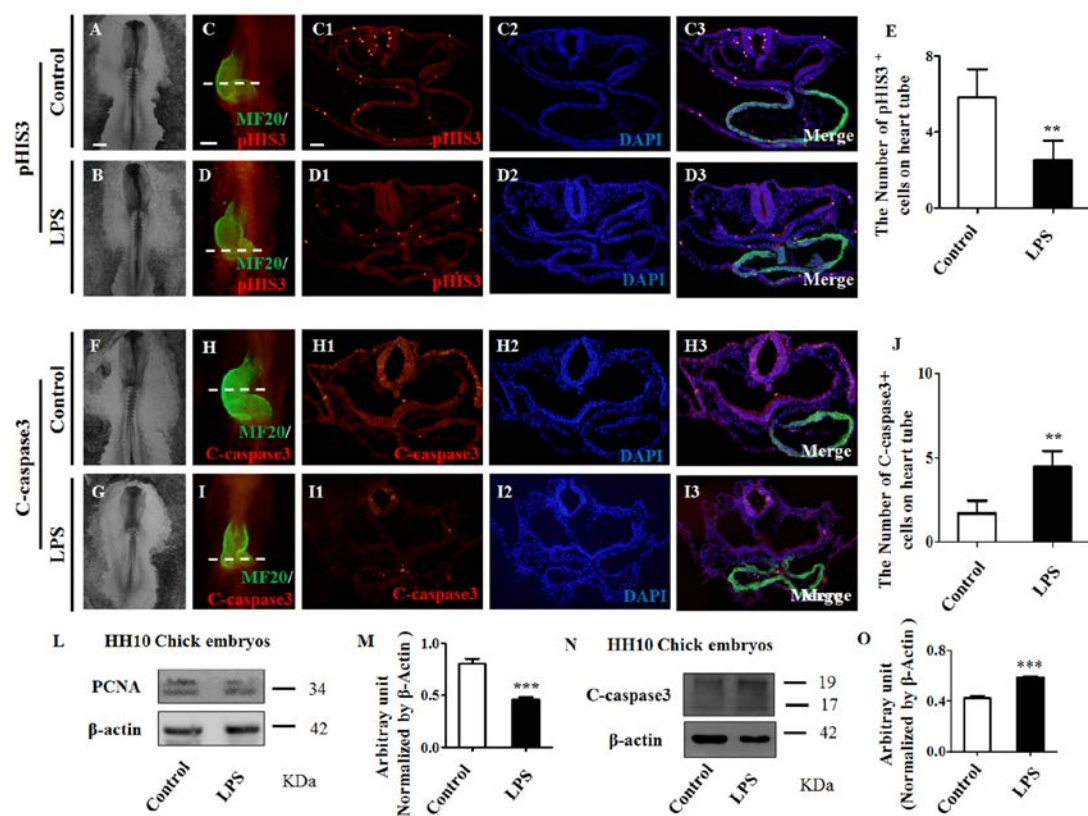


Figure 5

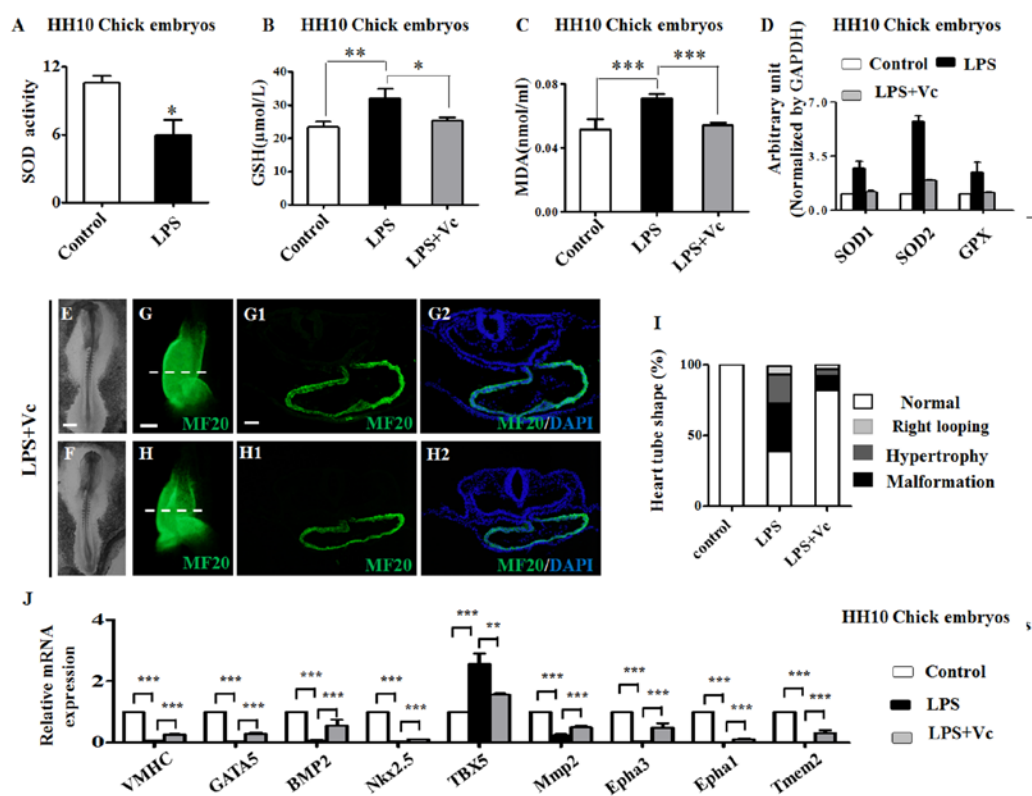


Figure 6

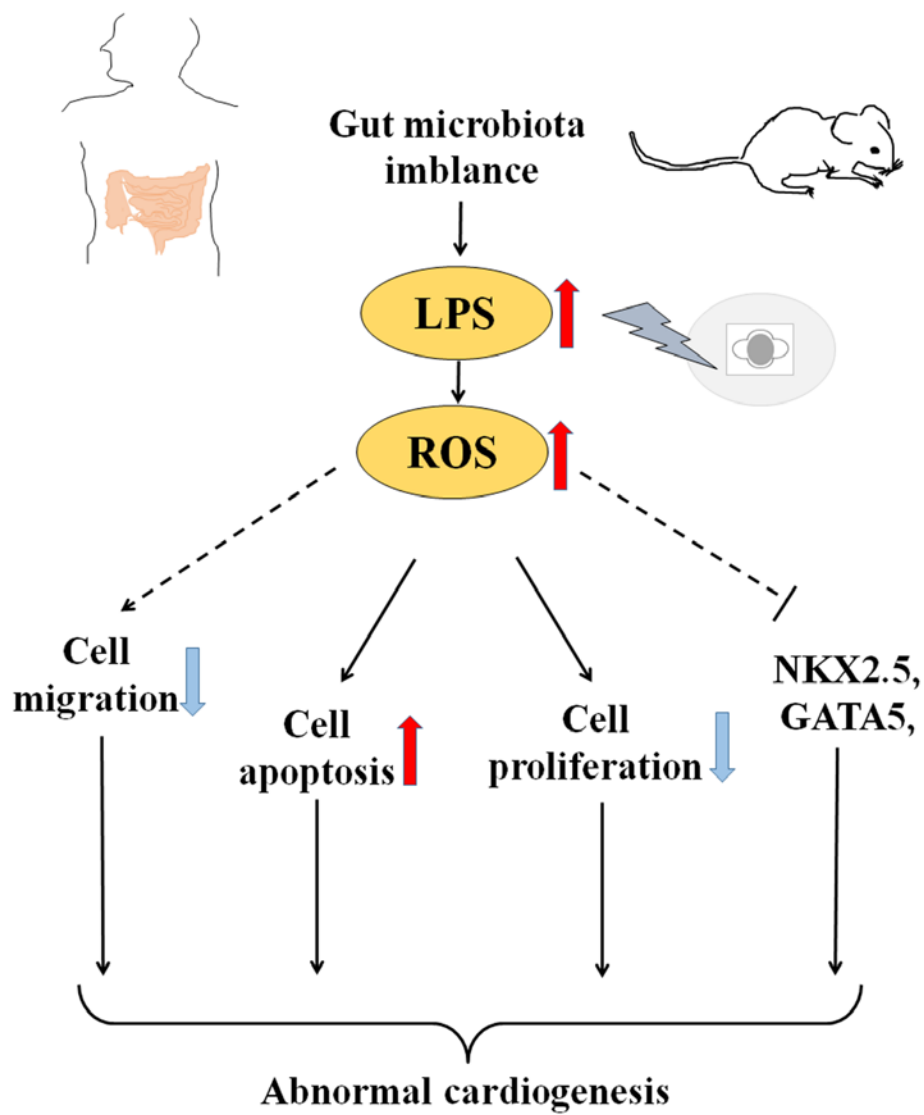


Figure 7